Scientia Iranica C (2014) 21(6), 2036–2048

SCIENTIA
IRANICA

Sharif University of Technology
Scientia Iranica
Transactions C: Chemistry and Chemical Engineering
www.scientiairanica.com

Adsorption of methyl-orange from aqueous solution onto nanoporous silica materials

M. Anbia[*] **and S. Salehi**

Research Laboratory of Nanoporous Materials, Faculty of Chemistry, Iran University of Science and Technology, Tehran, P.O. Box 16846, Iran.

Received 29 April 2013; received in revised form 12 September 2013; accepted 18 June 2014

KEYWORDS
Adsorption;
Mesoporous silica;
Methyl orange;
Polyelectrolyte;
Surfactant.

Abstract. The batch-adsorption experiments are carried out for anionic dye(methyl orange) using uncalcined mesoporous materials, calcined mesoporous materials and modified mesoporous materials by impregnation method using polyelectrolyte (PDDA, poly (diallydimethylammonium chloride) as a modification agent. The resulting samples were characterized by XRD, FT-IR and nitrogen adsorption-desorption analysis. The results indicate that uncalcined MCM-48 silica mesoporous molecular sieves (noted as MCM-48) can be used as the effective adsorbent for the removal of Methyl Orange (MO) from aqueous system. The effect of various factors such as chemical modification, contact time, initial concentration, adsorbent dose, agitation speed, and solution pH and reaction temperature has been studied. The experimental data obtained with MCM-48 fit best to the Langmuir isotherm model and exhibit a maximum adsorption capacity ($q_{\max}$) of 769.23 mg g^{-1}, and follows the second-order equation.

1. Introduction

Dyes are a class of organic compounds with complex aromatic molecular structure, which are discharged from many industries such as dyestuffs, textile, paper, printing, leather, cosmetics, plastics, paints, pharmaceuticals, food and petrochemicals [1,2]. Today more than 9000 types of dyes have been incorporated in the color index. Dyes can be classified as cationic (basic dyes), anionic (direct, acid, and reactive dyes) and non-ionic (disperse dyes) compounds [3]. Most of them have a complex aromatic molecular structure such as benzene, anthracene, naphthalene, xylene, toluene and so on [4]. The complex aromatic structures of dyes make them more stable to light, heat and oxidizing agents and are, therefore, difficult to degrade once released into aquatic systems. Many of these dyes are also toxic and even carcinogenic and this poses a serious hazard to aquatic living organisms and thus should be treated before discharging into the aqueous system [5].

Many treatment methods have been developed to remove dyes from wastewater, which can be divided into physical, chemical and biological methods, such as oxidation or ozonation [6], coagulation and flocculation [7], membrane separation [8] and adsorption [9]. These processes have their disadvantages and limitations, such as high cost, generation of secondary pollutants, and poor removal efficiency. Thus adsorption has been found to be the most effective economic alternative with high potential for the removal and recovery of dyes from wastewater [10]. This process transfers the dye species from the water effluent to a solid phase there by keeping the effluent volume to a minimum. Further, the adsorbent can be regenerated and the recovered dues can be property utilized without entering to the environment.

The emergence of porous silica materials with 2-50 nm ordered pore structure meets the increasing

---

[*] *Corresponding author. Tel.: +98 21 77240516;*
Fax: +98 21 77491204
E-mail address: anbia@iust.ac.ir (M. Anbia)

Table 1. The chemical structure and properties of methyl orange.

Dye	Molecular formula	Molecular weight (g/mol)	Structure	λ_{max} (nm)
Methyl Orange (MO)	$C_{14}H_{14}N_3O_3SNa$	327.30	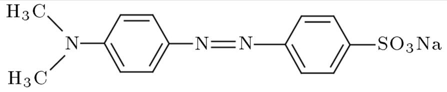	464

demands of applications involving large molecules in various fields. The milestones of the development of these types of materials were the development of M41s and SBA-x, which were synthesized under strong basic and acidic conditions, respectively [11,12]. Since then, various mesoporous materials such as MCM-48, MCM-41 and SBA-3 with different pore sizes and shapes were synthesized. The synthesis of MCM-48 (cubic *Ia*3*d*), MCM-41 (hexagonal *p*6*m*) and SBA-3 (hexagonal *p*6*m*) makes usage of cationic organic surfactants as the templates or structure directing agents. The large surface area and uniformity of pore size of mesoporous materials increase their application for separation and removal operations [13]. It is well known that mesoporous silicas have a negative charge density due to the presence of Si-O and Si-OH groups, which can adsorb positive charged dyes and does not permit the adsorption of negative ones [14]. In our group, cationic polyelectrolyte, PDDA (Poly(diallyldimethylammonium chloride)) was impregnated on MCM-48, MCM-41 and SBA-3, and thus prepared MCM-48/PDDA, MCM-41/PDDA and SBA-3/PDDA adsorbents which were used for the anionic dye adsorption. The modified mesoporous materials showed high adsorption capacity for anionic dye from aqueous solution, and the reason for this enhanced adsorption capacity for anionic dye might be due to the surface modification from anionic to cationic by impregnation of PDDA. In this study, mesoporous silicas were prepared and the surface has been modified with polyelectrolyte. In addition, the effect of surfactant template in MCM-48, MCM-41 and SBA-3 on the uptake of anionic dye (methyl orange) is studied. The changes in surface characteristics and pore structure of synthesized materials are characterized with FTIR, XRD and nitrogen adsorption-desorption isotherms. The effects of various parameters on the removal of anionic dye, such as chemical modification, contact time, initial concentration, adsorbent dose, agitation speed, solution pH and reaction temperature have been studied in detail. In addition, the equilibrium data are fitted into Langmuir and Freundlich equations to determine the correlation between the isotherm models and experimental data. The experimental data were also analyzed using the kinetic constants and first- and second-order kinetic model parameters were calculated.

2. Experimental

2.1. Materials

The tetraethylorthosilicate (TEOS), cetyltrimethylammonium bromide (CTAB), sodium hydroxide (NaOH), sodium fluoride (NaF), hydrochloric acid (HCl) and Methyl Orange (MO) were from E. Germany Merck. Low molecular weight PDDA (MW: 100,000 - 200,000 on average) was from Aldrich. All chemicals were of analytical grade. Aqueous solutions were prepared using distilled water. The chemical structure and properties of methyl orange are recorded in Table 1.

2.2. Methods

2.2.1. Synthesis of mesoporous silica (MCM-48)

In this work, mesoporous silica MCM-48 was synthesized by Shao method [15], using tetraethyl orthosilicate (TEOS) as the silica source and cetyltrimethylammonium bromide (CTAB) as a template. At first, 10 mL of TEOS was mixed with 50 mL of deionized water, and the mixture was vigorously stirred at 40°C for 40 minutes, then 0.9 g of NaOH and 0.19 g of NaF were added to this mixture. The solution was stirred for another 60 minutes and 10.61 g of CTAB was added to the solution, and stirring was continued for 60 minutes. The resulting mixture was transferred into a stainless-steel autoclave and maintained at 120°C under static conditions for 24 h for further condensation. A white precipitate (MCM-48) was recovered by filtration and washed extensively with deionized water and dried in an oven at 100°C. The removal of the organic template was done by calcination in the air at 550°C for 4 h (heating rate 1°C min^{-1}) to obtain the MCM-48/C.

2.2.2. Synthesis of mesoporous silica (MCM-41)

Mesoporous MCM-41 was prepared by adding 5.78 g of TEOS into a solution containing 1.01 g of CTAB and 0.34 g of NaOH in 30 mL of deionized water [16]. The resulting mixture was stirred at room temperature for 1 h and then was crystallized under the hydrothermal conditions at 110°C in a Teflon container for 96 h. The solid product (MCM-41) was obtained by filtration, and washed with deionized water. The product was then dried in the air and calcined.

2.2.3. Synthesis of mesoporous silica (SBA-3)

1 g of CTAB was dissolved in 47 mL of deionized water and acidified with 15 mL of concentrated HCl (Baker,

37%) to obtain a clear solution [17]. TEOS (4.45 mL) was added dropwise to the acidic CTAB solution stirring at 400 rpm at 30°C, and then the solution was left alone for 1 h. The solid product (SBA-3) was recovered by filtration and washed with deionized water and dried at 100°C overnight. To remove the organic surfactant template, the solid product was calcined, and the sample obtained was designated as SBA-3/C.

2.2.4. Synthesis of MCM-48 modified with polyelectrolyte (MCM-48/PDDA)

Modification of the prepared MCM-48 was performed as follows: MCM-48 was suspended in 0.1 M HCl (37%) solution to eliminate any contamination and also to increase the hydroxyl groups on the surface. The pretreated material was dried at an ambient temperature. 1 g of dried MCM-48 powder was immersed in 100 mL PDDA solution (5.0 wt%) and then mixture was stirred for 3h under ambient temperature. The resulting product (MCM-48/PDDA) was filtered and washed repeatedly with 100 mL deionized water. For the preparation of MCM-41/PDDA and SBA-3/PDDA, a similar process to that of the MCM-48/PDDA was used.

2.2.5. Material characterization

The porosity characteristics of the mesoporous materials were determined by N_2 adsorption-desorption experiments performed at 77 K on a micromeritics model ASAP 2010 sorptometer. The specific surface area was determined from the linear part of the isotherm curve using Brunauer-Emmet-Teller (BET) equation. Pore size distribution was estimated from the adsorption branch of the isotherm by the Barrett-Joyner-Halenda (BJH) method.

The FT-IR spectra for the mesoporous materials were measured on a DIGILAB FTS 7000 instrument under Attenuated Total Reflection (ATR) mode using a diamond module.

The X-Ray Diffraction (XRD) was used to identify the crystal phases of the mesoporous materials. These experiments were carried out on a Philips 1830 diffractometer equipped with Cu-Kα radiation. XRD patterns were obtained from 1° to 10° of 2θ, with a 2θ step size of 0.018° and a step time of 1 s.

2.3. Experiments

2.3.1. Adsorption studies

Adsorption behavior was studied by a batch method, which permits convenient evaluation of parameters that influence the adsorption process such as chemical modification, contact time, initial concentration, adsorbent dose, agitation speed, solution pH and reaction temperature. A series of aqueous solutions of dye with the same pH and their concentration ranging from 50 to 200 mg L^{-1} was prepared by dissolving a pure sample of the solute in double distilled water. In each adsorption experiment, 5 mg adsorbent was added in 25 mL dye solution. The solutions were stirred continuously at constant temperature. To observe the effect of pH, dye solutions with same initial concentration were adjusted to different pH (3-9) using 0.1 M NaOH and 0.1 M HCl solutions. To study the effect of temperature, the adsorption was carried out at four different temperatures (20, 40, 60 and 80°C) and for contact time studies the samples were taken at predetermined time intervals (5, 10, 15, 20, 25 and 30 minutes). To study the effect of agitation speed on the adsorption of dye varying agitation speeds from 0 to 300 rpm were examined. After adsorption, the residual concentration of dye in the filtrate was subsequently determined by the spectrophotometer at the wavelength corresponding to the maximum absorbance. The spectrophotometer was calibrated against standard solutions before each analysis. The amount of dye adsorbed per unit mass of the q_e (mg g^{-1}) was calculated by:

$$q_e = \frac{(C_0 - C_e)V}{W}, \tag{1}$$

where q_e is the adsorption capacity (mg g^{-1}) of the adsorbent at equilibrium, C_0 and C_e are the initial and equilibrium concentrations of solute (mg L^{-1}), respectively, V is the volume of the aqueous solution (L), and W is the mass (g) of adsorbent used in the experiments.

2.3.2. Adsorption kinetics of anionic dye

Adsorption kinetics experiments were made to investigate the effect of contact time and to determine the kinetic parameters. The adsorption kinetics of anionic dye onto adsorbent was investigated at one fixed initial concentration of dye (200 mg L^{-1}) by adding 25 mL dye solution to 0.005 g of adsorbent. The solution was stirred continuously (150 rpm) at 25°C. The samples at different time intervals (0-30 min) were taken and filtered. The residual concentration of dye in the filtrate was measured and the adsorption amount (q_t) was calculated by:

$$q_t = \frac{(C_0 - C_t)V}{W}, \tag{2}$$

where q_t is the measure of adsorption at time t, C_0 is the initial concentration of dye in the solution, C_t is the concentration of dye in the solution at time t, V is the volume of the solution, and W is the mass of adsorbent used in the experiments.

3. Results and discussion

3.1. Characterization of adsorbents

The quality and structural ordering of mesoporous materials were assessed by powder X-ray diffraction. The

XRD patterns of calcined and modified mesoporous materials are shown in Figure 1. XRD patterns of MCM-48/C exhibit two peaks at 2θ smaller than 3° and a series of weak peaks in the range of 3.5°-5.5° as expected for a MCM-48/C phase. They were assigned to the (211), (220), (420), (332), and (422) reflections, which belong to well-ordered cubic ($Ia3d$) pores. Three peaks at 2θ of 1.55°, 3.25° and 4.1° can be seen in the XRD pattern of MCM-41/C. Apparently, the hexagonally arranged channels, which are represented by (100), (110) and (200) reflections, exist in the MCM-41/C sample. The XRD patterns of SBA-3/C display three peaks at $2\theta = 2.76°$, 4.74° and 5.30°, respectively. These peaks were indexed as (100), (110) and (200) crystal facets, which belong to hexagonal ($P6m$) mesostructures. All these XRD reflection peaks are well resolved, indicating that these mesoporous materials have a high degree of ordering. The XRD reflection peaks for the modified mesoporous materials were retained after the modification by PDDA, but the intensities were slightly reduced that might be due to the partial damage of the mesoporous structure or due to the decreased contrast between walls and pores because of the cleavage of the silica species from the pore walls.

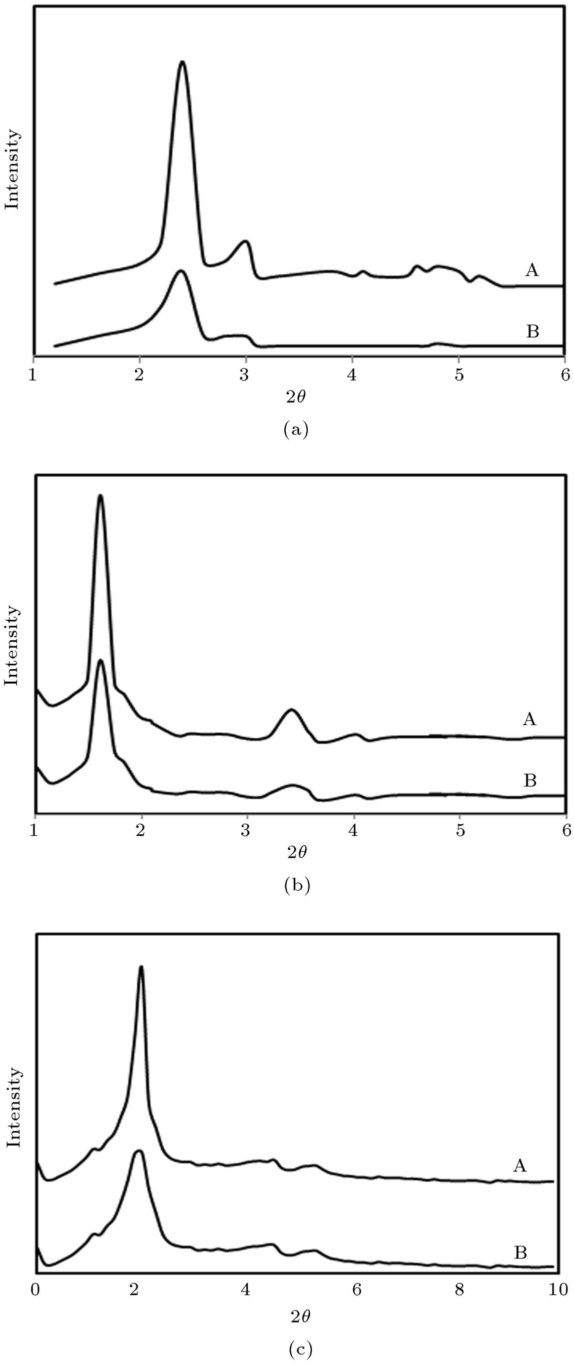

(a)

(b)

(c)

Figure 1. XRD patterns of (a) MCM-48/C (A) and MCM-48/PDDA (B), (b) MCM-41/C (A) and MCM-41/PDDA (B), and (c) SBA-3/C (A) and SBA-3/PDDA (B).

The texture characteristics of mesoporous materials were determined by the standard N_2 adsorption isotherms, followed by their analysis to evaluate the porosity parameters. This method provides information on the specific surface area and the pore diameter. Calculating pore diameters of mesoporous materials using the BJH equation is a usual method. Moreover, former studies have shown that the application of the BJH gives appropriate qualitative results which allows a direct comparison of relative changes between different mesoporous materials. Pores within porous materials are classified as micropores (< 2 nm), mesopores (2-50 nm), and macropores (> 50 nm), in accordance with the classification adopted by the IUPAC [18]. Figure 2 shows the isotherms of calcined and modified materials, which are also of the type IV. The type IV isotherm is typical for mesoporous systems [19]. N_2 adsorption-desorption measurements indicate that calcined and modified materials possess a good mesopore structure ordering and a relatively narrow pore size distribution. The textural parameters listed in Table 2 clearly confirm the structural changes of modified materials. From the above data, it becomes evident that the modification of the mesoporous materials with polyelectrolyte has induced a partial deformation of the ordered mesopore structure

Table 2. Textural properties determined from nitrogen adsorption-desorption experiments at 77 K.

Adsorbent	S_{BET} ($\mathrm{m^2g^{-1}}$)	**Average pore size (nm)**	V_P ($\mathrm{cm^3g^{-1}}$)
MCM-48/C	1340	2.24	1.04
MCM-48/PDDA	1180	2.19	0.91
MCM-41/C	1035	2.06	0.92
MCM-41/PDDA	975	2.01	0.78
SBA-3/C	1435	2.04	0.96
SBA-3/PDDA	1290	2.00	0.82

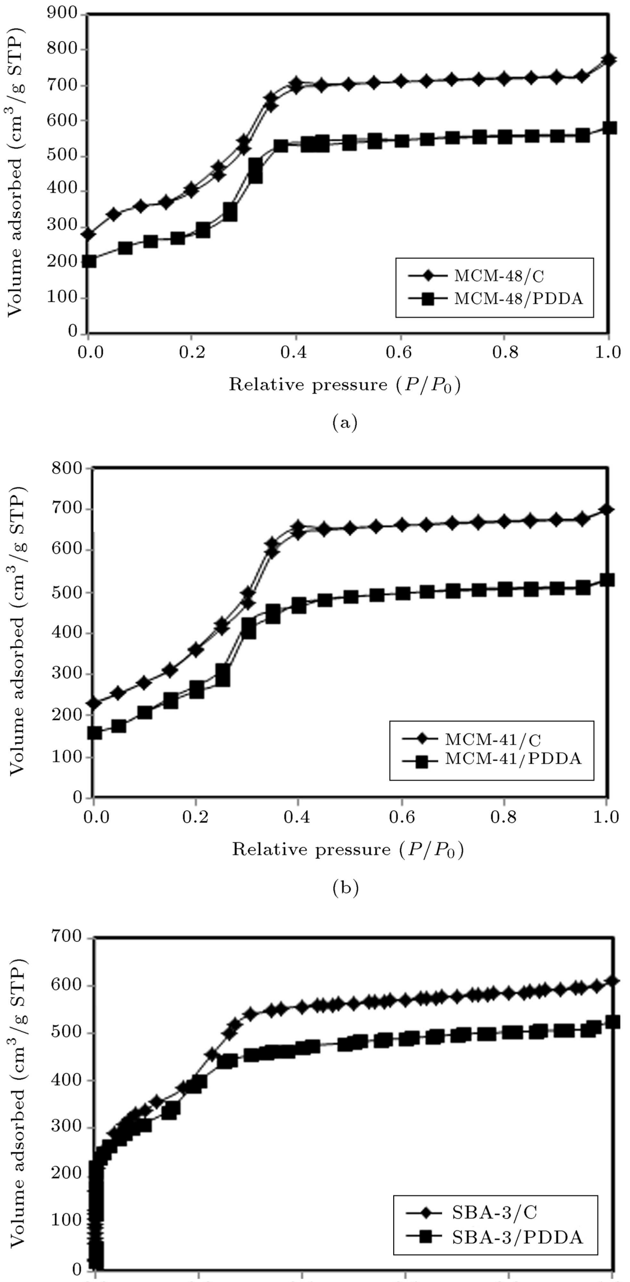

(a)

(b)

(c)

Figure 2. Adsorption-desorption isotherms of nitrogen at 77 K of MCM-48 (a), MCM-41(b) and SBA-3 (c).

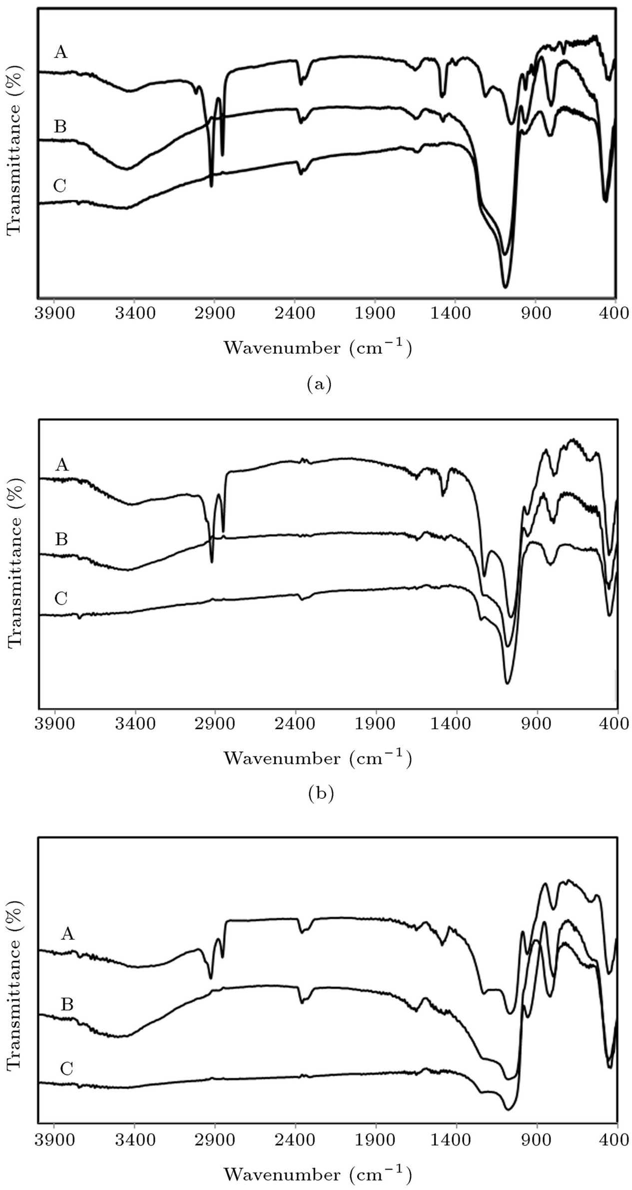

(a)

(b)

(c)

Figure 3. FT-IR spectra of (a) MCM-48 (A) MCM-48/PDDA (B) MCM-48/C (C), (b) MCM-41 (A) MCM-41/PDDA (B) MCM-41/C (C), and (c) SBA-3 (A) SBA-3/PDDA (B) SBA-3/C (C).

of the mesoporous materials, resulting in reduced BET surface area, average pore diameter and pore volume.

Qualitative identification of functional groups was accomplished by FT-IR spectroscopy. The FTIR spectrum is shown in Figure 3. A broad band in the range of 3700-3010 cm^{-1} is seen, which can be attributed to the framework of Si-OH group interaction with the defect sites and adsorbed water molecules. The Si-OH peak appears at about 3460 cm^{-1}, while peaks for the weak single Si-OH groups derived from the germinal Si-OH groups are observed at 3740 cm^{-1}. The asymmetric stretching vibrations of Si-O-Si and Si-OH are observed by the absorption bands at 1000-1360 cm^{-1} and the band at 790 cm^{-1} is assigned to free silica [20]. The uncalcined materials show that two very sharp intense bands at 2923 cm^{-1} and 2852 cm^{-1} correspond to the stretching of methyl and methylene groups, respectively [21], which are due to the presence of the organic surfactant molecules, and disappeared after the removal of the surfactant. After modification with PDDA, the broad band that appears at 1120 cm^{-1} is due to the symmetrical stretching of N-C bonds. Because of the induction effect of C joined with N, the

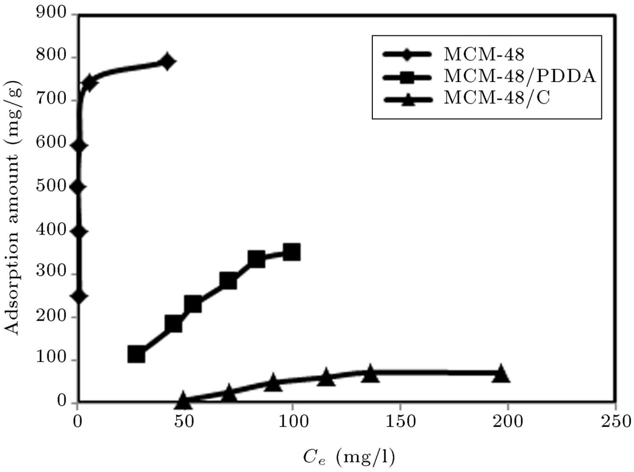

Figure 4. Adsorption isotherm for: MO adsorption on MCM-48 adsorbents (contact time = 30 min, adsorbent dosage = 0.2 gL^{-1}).

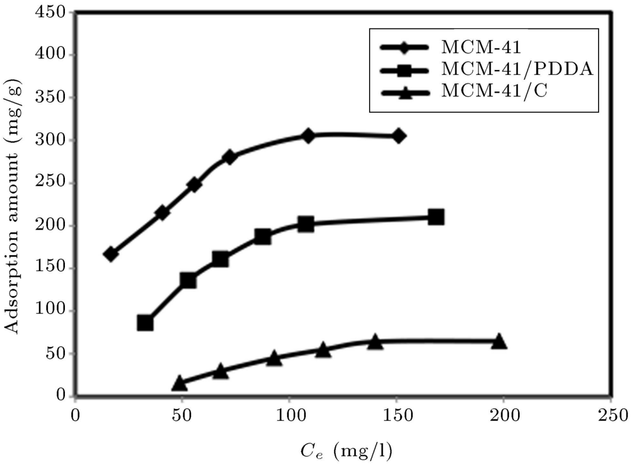

Figure 5. Adsorption isotherm for: MO adsorption on MCM-41 adsorbents (contact time = 30 min, adsorbent dosage = 0.2 gL^{-1}).

C-N stretching of amine is generally appeared at 1230-1030 cm^{-1} and can be considered in the region of a low wavenumber.

3.2. Effect of various parameters on adsorption

In the present study, MCM-48 is used for anionic dye removal from aqueous solutions. The effect of various important parameters such as contact time, initial concentration, adsorbent dose, agitation speed, solution pH and reaction temperature have been investigated.

3.2.1. Effect of chemical modification

In order to evaluate the efficacy of the prepared adsorbents, the equilibrium adsorption of the anionic dye is studied as a function of equilibrium concentration. The adsorption isotherms of MO on the adsorbents are shown in Figures 4-6. It is clear from these figures that the uncalcined mesoporous materials possess a higher adsorption capacity towards MO than the modified mesoporous materials. The existence of cationic template within the framework of uncalcined mesoporous materials causes a change in the surface chemistry and porosity of the adsorbents, which in turn affects the sorption behavior of the adsorbents [22]. The driving forces for the adsorption include a number of types such as dipole-dipole attractive force, van der Waals force, electrostatic interaction, hydrogen-bonding and hydrophobic interaction. There are multiple interactions among anionic dye and adsorbents due to the complex structure of the anionic dye. In the presence of CTAB in the mesoporous silica, the atomic cycles interact with the alkyl part of CTAB, while azo groups form hydrogen bonds with silanol groups on the internal surface of the mesoporous silica, and the sulfonic acid groups have an electrostatic attraction with positive heads of the surfactant. These multiple interactions give the surfactant-containing adsorbent excellent adsorption capability. The modified adsorbents exhibit a larger adsorption capacity than calcined adsorbents, which is due to electrostatic interaction. It is clear that the negative surface of the mesoporous silicas was successfully converted to a positive charge. Therefore, surface of mesoporous silicas change during modification with polyelectrolyte. Hence, significantly high electrostatic attractions exist between the positively charged surface of the adsorbent and the negatively charged dye ions, which can cause an increase in the adsorption of dye. The adsorption capacity of calcined adsorbents is weak and is generally due to the van der Waals interactions present between the molecules of dye and the walls of the mesopores [23]. MCM-48 has the highest adsorption capacity for the adsorption of MO, all other parameters are studied using this adsorbent.

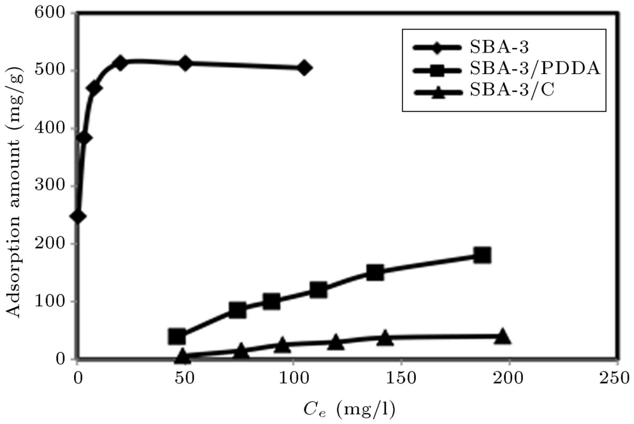

Figure 6. Adsorption isotherm for: MO adsorption on SBA-3 adsorbents (contact time = 30 min, adsorbent dosage = 0.2 gL^{-1}).

3.2.2. Effect of contact time and concentration

In order to establish an equilibration time for the maximum uptake and to evaluate the kinetics of the

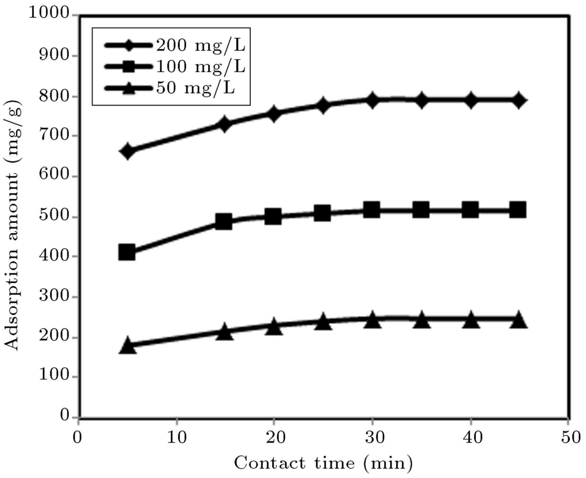

Figure 7. Effect of contact time and concentration for adsorption of MO on MCM-48 (adsorbent dosage = 0.2 gL^{-1}).

adsorption process, the adsorption of anionic dye on MCM-48 has been studied as a function of contact time. The results are shown in Figure 7. It is seen that the rate of uptake of the MO is rapid at the beginning and 50% of adsorption is completed within 10 min. Figure 7 also indicates that the time required for equilibrium is 30 min. Thus, for all equilibrium adsorption studies, the contact period was kept 30 min. As it can be seen in Figure 7, the adsorption capacity increases with an increase of initial anionic dye concentration. This may be due to the increase in the number of analyte molecules (or ions) competing for the available binding sites on the surface of the adsorbent. In addition, increase of initial anionic dye concentration increases the number of collisions between dye anions and the adsorbent, which enhances the adsorption process.

3.2.3. *Effect of adsorbent dose*

Adsorbent dose is an important parameter in the determination of adsorption capacity and adsorption percent. Figure 8 shows the effect of varying adsorbent dosage from 0.2 to 0.8 g/L of MCM-48. It is clear from this figure that initially the removal percentage increases rapidly with the increase in the adsorbent dose and after the critical dose the removal percentage almost reaches a constant value. An increase in adsorption percent with adsorbent dosage can be attributed to increased surface area and the availability of more adsorption sites [24]. However, the amount adsorbed per unit mass of the adsorbent decreases considerably. The decrease in adsorption capacity with increasing dose of adsorbent is basically due to the fact that the adsorption sites remain unsaturated during the adsorption process [25].

3.2.4. *Effect of agitation speed*

Agitation speed is also an important parameter in adsorption process, influencing the distribution of the solute in the bulk. The effect of agitation speed on removal efficiency of anionic dye has been studied by varying the speed of agitation from 0 (without shaking) to 300 rpm, while keeping the analyte concentration and contact time constant. As shown in Figure 9, the efficiency of MO removal increases with increasing agitation speed from 0 rpm to 150 rpm and the adsorption capacity remains constant for agitation rates greater than 150 rpm. Increasing the agitation rate causes the film resistance to mass transfer surrounding the adsorbent particles to decrease, resulting in an increase in the adsorption of the anionic dye molecules. The agitation speed of 150 rpm was selected as optimum speed.

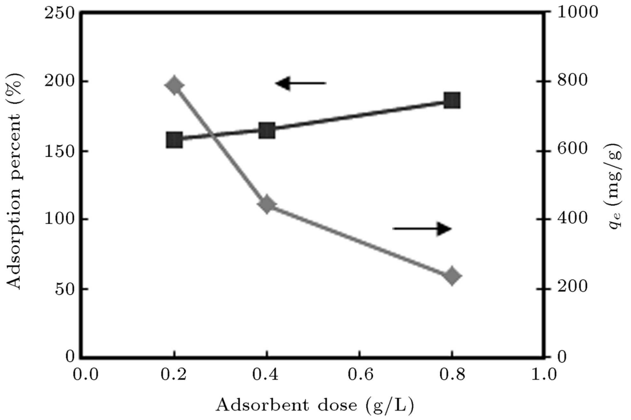

Figure 8. Effect of adsorbent dose for adsorption of MO on MCM-48 (initial concentration = 200 mgL^{-1}, contact time = 30 min).

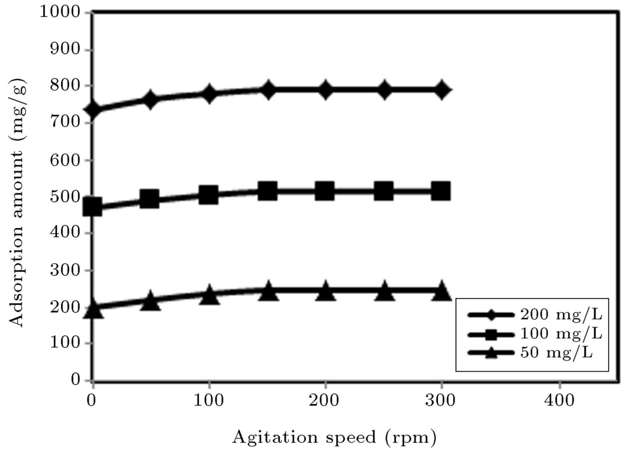

Figure 9. Effect of agitation speed for adsorption of MO on MCM-48 (contact time = 30 min, adsorbent dosage = 0.2 gL^{-1}).

3.2.5. *Effect of pH*

The adsorption capacity, the color of the dye solution and the solubility of some dyes are affected by pH. MO exists in a basic form when dissolved in aqueous solution. In acidic solution, its color changes from yellow to orange and finally to red with pH from 4.4 to 3.1 [26]. Figure 10 shows that maximum capacity

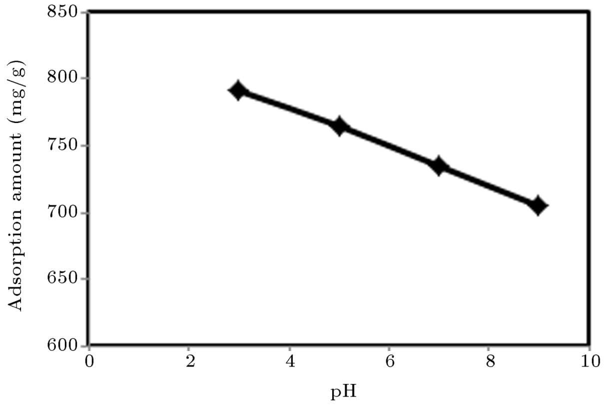

Figure 10. Effect of pH for adsorption of MO on MCM-48 (initial concentration = 200 mgL^{-1}, contact time = 30 min, adsorbent dosage = 0.2 gL^{-1}).

of MCM-48 is achieved in acidic condition at pH 3.0. With the increase of pH value, the capacity decreases. At lower pH, a significantly high electrostatic attraction exists between the positively charged surface of the adsorbent and negatively charged anionic dye [27]. At higher pH, the number of positively charged sites are reduced leading to increase in the number of negatively charged sites, creating electrostatic repulsion between the negatively charged surface of the MCM-48 and the anionic dye molecules. On the other hand, the lower adsorption of anionic dye, at alkaline pH, is because of the presence of excess OH$^-$ ions competing with the dye anions for the adsorption sites. As a result, there is a significant reduction in the adsorption of anionic dye from the solution. A similar behavior is reported for the adsorption of MO onto metal-organic frameworks [28].

3.2.6. Effect of temperature

Various textile dye effluents are produced at a relatively high temperature. Therefore, temperature can be an important factor for the real application of the MCM-48. The adsorption of MO on MCM-48 has been investigated as a function of temperature and maximum uptake value is obtained at 20°C as can be seen from Figure 11. This is attributed to the exothermic nature of this adsorption reaction. The enhancement in adsorption with temperature may be due to the physical bonding between anionic dye molecules and the active sites of the adsorbent. It is weakened as temperature increases, whereas, the solubility of dye increases, thus interaction between the solute and the solvent becomes stronger than those between solute and adsorbent, making the solute more difficult to adsorb. The adsorption is favoured by a decrease in temperature, a phenomenon which is also a characteristic of physical adsorption.

3.3. Adsorption isotherms

Adsorption isotherm is basically important to describe how solutes interact with adsorbents, and is critical in optimizing the use of adsorbents. Adsorption isotherm data of dyes are fitted to well-known and widely applied isotherm models of Langmuir and Freundlich. The Langmuir theory [29] is based on the assumption that adsorption takes place at specific homogeneous sites within the adsorbent and is used successfully in many monolayer adsorption process. The interactions between adsorbate and adsorbent are negligible. Its linearized form is given as

$$\frac{C_e}{q_e}=\frac{1}{q_m b}+\frac{1}{q_m}C_e, \tag{3}$$

where q_e is the amount of adsorbate adsorbed per unit mass of adsorbent (mg g^{-1}), C_e is the equilibrium concentration of the adsorbate (mgL^{-1}), and q_m (mgg^{-1}) and b (Lmg^{-1}) are the Langmuir constants related to maximum monolayer adsorption capacity and energy change in adsorption, respectively. The Freundlich equation [30] is based on adsorption on heterogeneous surfaces and is not restricted to the formation of the monolayer. Its linearized form is given as:

$$\ln q_e=\ln K_F+\left(\frac{1}{n}\right)\ln C_e, \tag{4}$$

where q_e is the amount of adsorbate adsorbed per unit mass of adsorbent (mg g^{-1}), C_e is the equilibrium concentration of the adsorbate (mg L^{-1}), K_F and n are Freundlich constants with n giving an indication of how favorable the adsorption process is, and K_F is the adsorption capacity of the adsorbent. When lnqe is plotted against $\ln C_e$ and the data are treated by linear regression analysis, K_F and $1/n$ constants are determined from the slope and intercept. The values of n and K_F can indicate whether the adsorption process is favourable or unfavourable.

The linearized Langmuir and Freundlich isotherm gives satisfying fit of equilibrium data as shown in Figure 12(a) and (b), respectively. The parameters

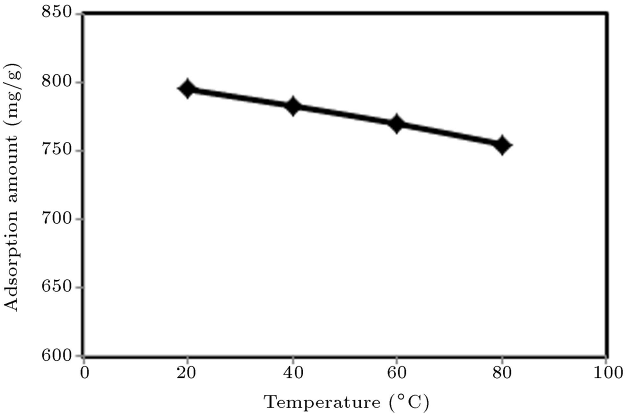

Figure 11. Effect of temperature for adsorption of MO on MCM-48 (initial concentration = 200 mgL^{-1}, contact time = 30 min, adsorbent dosage = 0.2 gL^{-1}).

Table 3. Isotherm parameters for adsorption of MO on MCM-48.

Dye	Langmuir			Freundlich		
	q_m (mg/g)	b (L/mg)	R^2	K_F [(mg g^{-1}) (mg^{-1})$^{1/n}$]	n (L mg^{-1})	R^2
MO	769.23	4.33	0.9999	381.45	2.34	0.9720

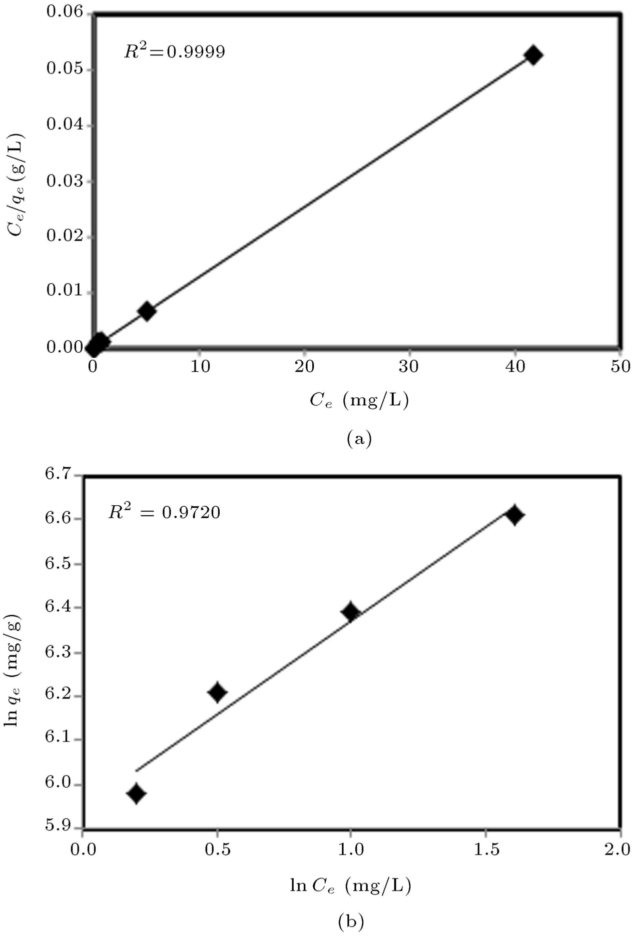

(a)

(b)

Figure 12. Adsorption isotherm for removal of MO by MCM-48: (a) Langmuir and (b) Freundlich isotherm (initial concentration = 50-200 mgL^{-1}, contact time = 30 min, adsorbent dosage = 0.2 gL^{-1}).

of these equations obtained by linear regression analysis of the experimentally derived data are given in Table 3 together with regression coefficients, R^2. The R^2 values of the Langmuir and Freundlich isotherms are 0.999 and 0.972, respectively, indicating that the equilibrium sorption data fit better with the Langmuir isotherm. In addition, the high value of correlation coefficient ($R^2 > 999$) on Langmuir adsorption isotherm indicates that the monolayer adsorption occurs by electrostatic interaction between MCM-48 and MO [31].

3.4. Adsorption kinetics

The factors affecting the reaction rates for the adsorption of anionic dye on MCM-48 are studied through adsorption kinetic experiments. Any adsorption process is normally controlled by three diffusion steps:

(i) Solute transport from bulk solution to the film surrounding the adsorbent;

(ii) From the film to the adsorbent surface;

(iii) From the surface to the internal sites followed by binding of the metal ions to the active sites.

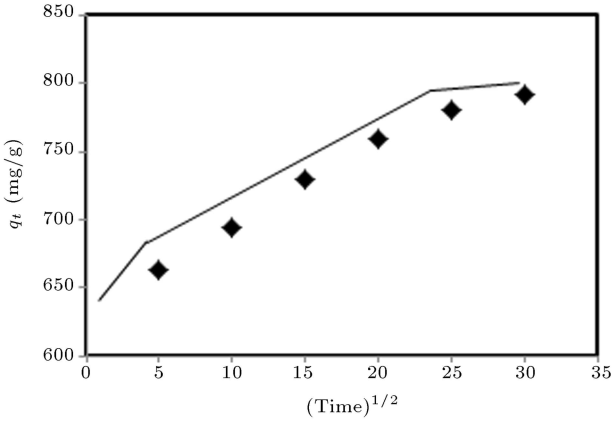

Figure 13. Plot of q_t vs. t for adsorption MO on MCM-48.

The overall rate of the adsorption process is determined by the slowest step, and usually it is thought that step (ii) leads to surface adsorption and step (iii) leads to intra-particle adsorption [32].

Figure 13 presents the typical plots for the adsorption of MO on MCM-48 using diffusion model. The diffusion of anionic dye from the solution to the exterior surface of adsorbent causes the first curved portion, which starts at onset of the process and is the fastest. The molecular dye enters into the pores of MCM-48 particles and is adsorbed by the interior surface of the particles when the exterior surface reaches to saturation. The diffusion into wider mesopores is responsible for the second part of the plot while the third part of the plot with the lowest slope relates to adsorption in narrow mesopores. Several adsorption kinetic models are available in this work, the pseudo-first-order Lagergren equation and pseudo second-order rate equation are fitted with the experimental data. The pseudo-first order rate expression is generally described by [33]:

$$\log(q_e - q_t) = \log q_e - \left(\frac{K_1}{2.303}\right) t, \tag{5}$$

Table 4. Kinetics parameters for adsorption of MO on MCM-48.

Dye	**Pseudo-first kinetic**			**Pseudo-second-order kinetic**		
	q_e (mg/g)	K_1 (min)$^{-1}$	R^2	q_e (mg/g)	K_2 (g/mgm)	R^2
MO	251.21	0.10	0.9527	833.33	0.001	0.9978

Table 5. Comparison of adsorption capacity of MO onto various adsorbents.

Adsorbent	**Temperature (°C)**	q_m **(mg/g)**	**Reference**
Activated alumina	25	9.8	[36]
MUCP (Modified Ultrafine Coal Powder)	30	18.52	[37]
Banana peel	30	21.0	[38]
Orange peel	30	20.5	[38]
De-oiled soya	30	13.4	[39]
Bottom ash	30	13.3	[39]
MWCNTs (multiwalled carbon nanotubes)	25	51.74	[40]
HJ-1 (hypercross linked polymeric adsorbent)	20	70.92	[41]
MSE (Modified Silkworm Exuviae)	30	87.03	[42]
CCM (Carbon Coated Monolith)	30	102.04	[43]
Chitosan	25	130	[44]
CTMAB/10SSTA-MMT (modified montmorillonite)	30	149.25	[45]
Zn/Al-LDO (calcined layered double hydroxides)	25	200.0	[46]
PAAC (phragmitesaustralis activated carbon)	10	238.10	[47]
Activated carbon	25	11.2	[28]
MIL-53	25	57.9	[28]
MIL-101	25	114.0	[28]
ED-MIL-101 (ethylenediamine-grafted MIL-101)	25	160.0	[28]
PED-MIL-101 (protonated ethylenediamine-grafted MIL-101)	25	194.0	[28]
LVM (Lapindo Volcanic Mud)	30	333.33	[48]
γ-Fe_2O_3	25	385.0	[49]
SBA-3	25	357.1	[9]
Mesoporous TiO_2	-	454.5	[50]
MOF-235 (metal-organic framework)	25	477.0	[51]
MCM-48	25	769.23	Present study

where q_e and q_t are the adsorption capacities at equilibrium and at time t, respectively (mg g^{-1}), and k_1 is the rate constant of pseudo-first order adsorption (min^{-1}). The pseudo-second-order rate equation can be explained by the equation [34]:

$$\frac{t}{q_t} = \frac{1}{K_2 q_e^2} + \left(\frac{1}{q_e}\right) t, \tag{6}$$

where the pseudo second order constants k_2 (g (mg min)$^{-1}$), and the equilibrium adsorption capacity q_e can be determined experimentally from the slope and intercept of the plot t/q_t versus t. The pseudo first order kinetics are generally used to describe the initial stage of the adsorption process. However, pseudo-second-order kinetics is based on the adsorption capacity, which usually gives a good description of the whole adsorption process. From Table 4, it is clear that the pseudo-second-order kinetic model gives a better correlation for the adsorption of MO on MCM-48 compared to the pseudo-first-order model. A similar result was obtained for the adsorption of various acidic and basic dyes onto activated carbon cloth [35].

3.5. Comparison with other adsorbents

The value of $q_{\max}$ is important to identify which sorbent shows the highest adsorption capacity and is useful in scale-up considerations. Table 5 shows the comparison of adsorbent capacity of various adsorbents for MO. When compared with other adsorbents, the results of the present study indicate that MCM-48 has a large adsorption capacity (769.23 mg g^{-1}), suggesting that it may be a promising material for the removal of MO from aqueous solutions.

4. Conclusions

In this study, adsorption properties of on anionic dye by mesoporous silica materials have been studied. The obtained results have shown that the adsorption capacity of the adsorbents varies in the order of uncalcined mesoporous materials>modified mesoporous materials>calcined mesoporous materials. The higher adsorption capacity of uncalcined materials may be due to the fact that the polar groups created by surfactant template present on the uncalcined mesoporous materials surface imparted considerable anions adsorption capacity to it. The cationic polyelectrolyte, PDDA, was impregnated on mesoporous silicas and the surface charges of the mesoporous silicas were easily converted from negative to positive by a simple method. In addition, the PDDA impregnated silica adsorbent could adsorb anionic dye because of the electrostatic attractions. Our results demonstrate that MCM-48 can be used as the effective adsorbent for the removal of Methyl Orange (MO) from aqueous solution.

Acknowledgment

The authors are thankful to Research Council of Iran University of Science and Technology (Tehran) for financial support.

References

1. Kajiyama, S., Uemura, Y., Miura, H., Hara, K. and Koumura N. "Organic dyes with oligo-n-hexylthiophene for dye-sensitized solar cells: Relation between chemical structure of donor and photovoltaic performance", *Dyes Pigm.*, **92**, pp. 1250-1256 (2012).
2. Okada, Y., Hihara, T. and Morita, Z. "Analysis of photofading of phenylazo-indole and phenylazo-N-ethanolaniline disperse dyes on poly(ethylene terephthalate) fabric using the PM5 method", *Dyes Pigm.*, **83**, pp. 237-248 (2009).
3. Allen, R.L.M., *Color Chemistry*, New York, Appleton-Century-Crofts (1971).
4. Alkan, M., Demirbas, Ö., Celikcapa, S. and Dogan, M. "Sorption of acid red 57 from aqueous solution onto sepiolite", *J. Hazard. Mater.*, **116**, pp. 135-145 (2004).
5. Ajji, Z. and Ali, A.M. "Adsorption of methyl violet and brilliant blue onto poly (vinyl alcohol) membranes grafted with N-vinyl imidazole/acrylic acid", *Nucl. Instrum. Methods. Phys. Res. Sect B*, **265**, pp. 362-365 (2007).
6. Gao, M., Zeng, Z., Sun, B., Zou, H., Chen, J. and Shao, L. "Ozonation of azo dye acid red 14 in a microporous tube-in-tube microchannel reactor: Decolorization and mechanism", *Chemosphere*, **89**, pp. 190-197 (2012).
7. Moghaddam, S.S., Moghaddam, M.R. and Arami, A. "Coagulation/flocculation process for dye removal using sludge from water treatment plant: Optimization through response surface methodology", *J. Hazard. Mater.*, **175**, pp. 651-657 (2010).
8. Damodar, R.A., You, S.J. and Ou, S.H. "Coupling of membrane separation with photocatalytic slurry reactor for advanced dye wastewater treatment", *Sep. Purif. Technol.*, **76**, pp. 64-71 (2010).
9. Anbia, M., Harriri, S.A. and Ashrafizadeh, S.N. "Adsorptive removal of anionic dyes by modified nanoporous silica SBA-3", *Appl. Surf. Sci.*, **256**, pp. 3228-3233 (2010).
10. Han, R., Wang, Y., Zou, W., Wang, Y. and Shi, J. "Comparison of linear and nonlinear analysis in estimating the Thomas model parameters for methylene blue adsorption onto natural zeolite in fixed-bed column", *J. Hazard. Mater.*, **145**, pp. 331-335 (2007).
11. Anbia, M. and Lashkari, M. "Synthesis of amino-modified ordered mesoporous silica as a new nanosorbent for the removal of chlorophenols from aqueous media", *Chem. Eng. J.*, **150**, pp. 555-560 (2009).
12. Anbia, M., Mohammadi, N. and Mohammadi, K. "Fast and efficient mesoporous adsorbents for the separation of toxic compounds from aqueous media", *J. Hazard. Mater.*, **176**, pp. 965-972 (2010).
13. Tanev, P.T. and Pinnavaia, T.J. "A neutral templating route to mesoporous molecular sieves", *Science*, **267**, pp. 865-867 (1995).
14. Saad, R., Belkacemi, K. and Hamoudi, S. "Adsorption of phosphate and nitrate anions on ammonium-functionalized MCM-48: Effects of experimental conditions", *J. Colloid. Interface. Sci.*, **311**, pp. 375-381 (2007).
15. Shao, Y., Wang, L., Zhang, J. and Anpo, M. "Synthesis of hydrothermally stable and longrange ordered Ce-MCM-48 and Fe-MCM-48 materials", *Micropor. Mesopor. Mater.*, **109**, pp. 20835-20841 (2005).
16. Chen, H. and Wang, Y. "Preparation of MCM-41 with high thermal stability and complementary textural porosity", *Ceram. Int.*, **28**, pp. 541-547 (2002).
17. Göltner, C.G., Smarsly, B., Berton, B. and Antonietti, M. "On the microporous nature of mesoporous molecular sieves", *Chem. Mater.*, **13**, pp. 1617-1623 (2001).
18. Duman, O. and Ayranci, E. "Adsorption characteristics of benzaldehyde, sulphanilic acid and p-phenolsulfonate from water, acid or base solutions on

to activated carbon cloth", *Sep. Sci. Technol.*, **41**, pp. 3673-3692 (2006).

19. Sing, K.S.W., Everett, D.H., Haul, R.A.W., Mouscou, L., Pierotti, R.A, Rouquerol, J. and Siemieniewska, T. "Reporting physisorption data for gas/solid systems with special reference to the determination of surface area and porosity", *Pure. Appl. Chem.*, **57**, pp. 603-619 (1985).
20. Ghiaci, M., Abbaspur, A., Kia, R., Belver, C., Trujillano, R., Rives, V. and Vicente, M.A. "Vapor-phase alkylation of toluene by benzyl alcohol on H_3PO_4-modified MCM-41 mesoporous silicas", *Catal. Commun.*, **8**, pp. 49-56 (2007).
21. Duman, O., Tunç, S. and Çetinkaya, A. "Electrokinetic and rheological properties of kaolinite in poly(diallyldimethylammonium chloride), poly(sodium 4-styrene sulfonate) and poly(vinyl alcohol) solutions", *Colloid Surfaces A*, **394**, pp. 23-32 (2012).
22. Kleitz, F., Schmidt, W. and Schüth, F. "Evolution of mesoporous materials during the calcinations process: Structural and chemical behavior", *Micropor. Mesopor. Mater.*, **44**, pp. 95-109 (2001).
23. Zhao, Y.X., Ding, M.Y. and Chen, D.P. "Adsorption properties of mesoporous silicas for organic pollutants in water", *Anal. Chim. Acta.*, **542**, pp. 193-198 (2005).
24. Garg, V.K., Gupta, R., Yadav, A.B. and Kumar, R. "Dye removal from aqueous solution by adsorption on treated sawdust", *Bioresour. Technol.*, **89**, pp. 121-124 (2003).
25. Garg, V.K., Amita, M., Kumar, R. and Gupta, R. "Basic dye (methylene blue) removal from simulated wastewater by adsorption using Indian Rosewood sawdust: a timber industry waste", *Dyes Pigm.*, **63**, pp. 243-250 (2004).
26. Zhang, A. and Fan, Y. "Influence of adsorption orientation of methyl orange on silver colloids by Raman and fluorescence spectroscopy: pH effect", *Chem. Phys.*, **331**, pp. 55-60 (2006).
27. Kadirvelu, K., Karthika, C., Vennilamani, N. and Pattabi, S. "Activated carbon from industrial solid waste as an adsorbent for the removal of Rhodamine-B from aqueous solution: Kinetic and equilibrium studies", *Chemosphere*, **60**, pp. 1009-1017 (2005).
28. Haque, E., Lee, J.E., Jang, I.T., Hwang, Y.K., Chang, J.S., Jegal, J. and Jhung, S.H. "Adsorptive removal of methyl orange from aqueous solution with metal-organic frameworks, porous chromium-benzenedicarboxylates", *J. Hazard. Mater.*, **181**, pp. 535-542 (2010).
29. Langmuir, I. "Adsorption of gases on plain surfaces of glass mica platinum", *J. Am. Chem. Soc.*, **40**, pp. 136-403 (1918).
30. Freundlich, H.M.F. "Over the adsorption in solution", *J. Phys. Chem.*, **57**, pp. 385-470 (1906).
31. Rengaraj, S., Yeon, J.W., Kim, Y., Jung, Y., Ha, Y.K. and Kim, W.H. "Adsorption behavior of Cu (II) onto ion exchange resins 252H and 1500H: kinetics, isotherms and error analysis", *J. Hazard. Mater.*, **143**, pp. 469-477 (2007).
32. Babu, B.V. and Gupta, S. "Adsorption of Cr (VI) using activated neem leaves: kinetic studies", *Adsorption*, **14**, pp. 85-92 (2008).
33. Ho, Y.S., Ng, J.C.Y. and McKay, G. "Kinetics of pollutant sorption by biosorbents: Review", *Sep. Purif. Methods*, **29**, pp. 189-232 (2000).
34. McKay, G. and Ho, Y.S. "Pseudo-second order model for sorption processes", *Process. Biochem.*, **34**, pp. 451-465 (1999).
35. Ayranci, E. and Duman, O. "In-situ UV-visible spectroscopic study on the adsorption of some dyes onto activated carbon cloth", *Sep. Sci. Technol.*, **44**, pp. 3735-3752 (2009).
36. Iida, Y., Kozuka, T., Tuziuti, T. and Yasui, K. "Sonochemically enhanced adsorption and degradation of methyl orange with activated aluminas", *Ultrasonics*, **42**, pp. 635-639 (2004).
37. Zhuannian, L., Anning, Z., Guirong, W. and Xiaoguang, Z. "Adsorption behavior of methyl orange onto modified ultrafine coal powder", *Chin. J. Chem.*, **17**, pp. 942-948 (2009).
38. Annadurai, G., Juang, R.S. and Lee, D.J. "Use of cellulose-based wastes for adsorption of dyes from aqueous solutions", *J. Hazard. Mater.*, **92**, pp. 263-274 (2002).
39. Mittal, A., Malviya, A., Kaur, D., Mittal, J. and Kurup, L. "Studies on the adsorption kinetics and isotherms for the removal and recovery of methyl orange from wastewaters using waste materials", *J. Hazard. Mater.*, **148**, pp. 229-240 (2007).
40. Yao, Y., He, B., Xu, F. and Chen, X. "Equilibrium and kinetic studies of methyl orange adsorption on multi walled carbon nanotubes", *Chem. Eng. J.*, **170**, pp. 82-89 (2011).
41. Huang, J.H., Huang, K.L., Liu S.Q., Wang, A.T. and Yan, C. "Adsorption of Rhodamine B and methyl orange on a hypercrosslinked polymeric adsorbent in aqueous solution", *Colloid Surface Physicochem. Eng. Aspect.*, **330**, pp. 55-61 (2008).
42. Chen, H., Zhao, J., Wu, J. and Dai, G. "Isotherm, thermodynamic, kinetics and adsorption mechanism studies of methyl orange by surfactant modified silkworm exuviae", *J. Hazard. Mater.*, **192**, pp. 246-254 (2011).
43. Hosseini, S., Khan, M.A., Malekbala, M.R., Cheah, W. and Choong, T.S.Y. "Carbon coated monolith, a mesoporous material for the removal of methyl orange from aqueous phase: Adsorption and desorption studies", *Chem. Eng. J.*, **171**, pp. 1124-1131 (2011).
44. Morias, W.A., Fernandes, A.L.P., Dantas, T.N.C.,

Pereira, M.R. and Fonseca, J.L.C. "Sorption studies of a model anionic dye on crosslinked chitosan", *Colloid Surface Physicochem. Eng. Aspect.*, **310**, pp. 20-31 (2007).

45. Chen, D., Chen, J., Luan, X., Ji, H. and Xia, Z. "Characterization of anion-cationic surfactants modified montmorillonite and its application for the removal of methyl orange", *Chem. Eng. J.*, **171**, pp. 1150-1158 (2011).

46. Ni, Z.M., Xia, S.J., Wang, L.G., Xing, F.F. and Pan, G.X. "Treatment of methyl orange by calcined layered double hydroxides in aqueous solution: Adsorption property and kinetic studies", *J. Colloid. Interface. Sci.*, **316**, pp. 284-291 (2007).

47. Chen, S., Zhang, J., Zhang, C., Yue, Q., Li, Y. and Li, C. "Equilibrium and kinetic studies of methyl orange and methyl violet adsorption on activated carbon derived from Phragmitesaustralis", *Desalination*, **252**, pp. 149-156 (2010).

48. Jalil, A.A., Triwahyono, S., Adam, S.H., Rahim, N.D., Aziz, M.A.A., Hairom, N.H.H., Razali, N.A.M., Abidin, M.A.Z. and Mohamadiah, M.K.A. "Adsorption of methyl orange from aqueous solution onto calcined Lapindo volcanic mud", *J. Hazard. Mater.*, **181**, pp. 755-762 (2010).

49. Asuha, S., Gao, Y.W., Deligeer, W., Yu, M., Suyala, B. and Zhao, S. "Adsorptive removal of methyl orange using mesoporous maghemite", *J. Porous. Mater.*, **18**, pp. 581-587 (2011).

50. Asuha, S., Zhou, X.G. and Zhao, S. "Adsorption of methyl orange and Cr(VI) on mesoporous TiO_2 prepared by hydrothermal method", *J. Hazard. Mater.*, **181**, pp. 204-210 (2010).

51. Haque, E., Jun, J.W. and Jhung, S.H. "Adsorptive removal of methyl orange and methylene blue from aqueous solution with a metal-organic framework material, iron terephthalate (MOF-235)", *J. Hazard. Mater.*, **185**, pp. 507-511 (2011).

Biographies

Mansoor Anbia obtained his MSc from Tehran Tarbiat Moallem University doing a case study on "Synthesis, properties and applications of lanthanum silicates as mineral ion-exchangers". He then did a Post MSc research on "Measuring ^{222}Rn content of mineral water employing alpha-spectroscopy and liquid scintillation method" at the same University. He also earned his PhD from Tehran Tarbiat Moallem University in 2007 under the supervision of Professor Vaghef Hossein. His thesis was entitled "Case study on synthesis, properties and analytical applications of novel mesoporous compounds of lanthanum silicate, lanthanum phosphate, lanthanum tantalate and titanium phosphate".

Dr. Anbia has been honored with several national and international scientific awards. He is currently an associate professor at Iran University of Science and Technology and at the same time the President of the Chemistry and Chemical Engineering Research Center of Iran. His research interests include inorganic ion-exchangers, mesoporous adsorbents, nano structure new materials, chromatography (HTPLC, HPLC & GSC), removal of organic and inorganic pollutants from industrial effluents, purification methods for recovery of different chemical compounds from industrial waste, and application of new materials for using in different industrial plants.

Samira Salehi obtained her BSc from Islamic Azad University, Shahre Qods Branch. She also earned her MSc from Iran University of Science and Technology in 2011 under the supervision of Professor Mansoor Anbia. Her thesis was entitled "Synthesis and characterization of carbon nanostructure modified with organic functional groups and its application as a new adsorbent for removal of acidic compounds from oil industries procedure".